

Circulation Research

JOURNAL OF THE AMERICAN HEART ASSOCIATION

American Heart
Association® 
Learn and Live™

Discoidin Domain Receptor 1 on Bone Marrow Derived Cells Promotes Macrophage Accumulation During Atherogenesis

Christopher Franco, Karen Britto, Eric Wong, Guangpei Hou, Su-Ning Zhu, Mian
Chen, Myron I. Cybulsky and Michelle P. Bendeck

Circ. Res. 2009;105;1141-1148; originally published online Oct 15, 2009;

DOI: 10.1161/CIRCRESAHA.109.207357

Circulation Research is published by the American Heart Association, 7272 Greenville Avenue, Dallas,
TX 75214

Copyright © 2009 American Heart Association. All rights reserved. Print ISSN: 0009-7330. Online
ISSN: 1524-4571

The online version of this article, along with updated information and services, is
located on the World Wide Web at:

<http://circres.ahajournals.org/cgi/content/full/105/11/1141>

Data Supplement (unedited) at:

<http://circres.ahajournals.org/cgi/content/full/CIRCRESAHA.109.207357/DC1>

Subscriptions: Information about subscribing to Circulation Research is online at
<http://circres.ahajournals.org/subscriptions/>

Permissions: Permissions & Rights Desk, Lippincott Williams & Wilkins, a division of Wolters
Kluwer Health, 351 West Camden Street, Baltimore, MD 21202-2436. Phone: 410-528-4050. Fax:
410-528-8550. E-mail:
journalpermissions@lww.com

Reprints: Information about reprints can be found online at
<http://www.lww.com/reprints>

Discoidin Domain Receptor 1 on Bone Marrow–Derived Cells Promotes Macrophage Accumulation During Atherogenesis

Christopher Franco, Karen Britto, Eric Wong, Guangpei Hou, Su-Ning Zhu, Mian Chen, Myron I. Cybulsky, Michelle P. Bendeck

Rationale: We described a critical role for the discoidin domain receptor (DDR)1 collagen receptor tyrosine kinase during atherosclerotic plaque development. Systemic deletion of *Ddr1* in *Ldlr*^{-/-} mice accelerated matrix accumulation and reduced plaque size and macrophage content. However, whether these effects reflected an independent role for macrophage DDR1 during atherogenesis remained unresolved.

Methods: In the present study, we performed sex-mismatched bone marrow transplantation using *Ddr1*^{+/+}; *Ldlr*^{-/-} and *Ddr1*^{-/-}; *Ldlr*^{-/-} mice to investigate the role of macrophage DDR1 during atherogenesis. Chimeric mice with deficiency of DDR1 in bone marrow–derived cells (*Ddr1*^{-/-→+/+}) or control chimeric mice that received *Ddr1*^{+/+}; *Ldlr*^{-/-} marrow (*Ddr1*^{+/+→+/+}) were fed an atherogenic diet for 12 weeks.

Results: We observed a 66% reduction in atherosclerosis in the descending aorta and a 44% reduction in plaque area in the aortic sinus in *Ddr1*^{-/-→+/+} mice compared to *Ddr1*^{+/+→+/+} mice. Furthermore, we observed a specific reduction in the number of donor-derived macrophages in *Ddr1*^{-/-→+/+} plaques, suggesting that bone marrow deficiency of DDR1 attenuated atherogenesis by limiting macrophage accumulation in the plaque. We have also demonstrated that the effects of DDR1 on macrophage infiltration and accumulation can occur at the earliest stage of atherogenesis, the formation of the fatty streak. Deficiency of DDR1 limited the appearance of 5-bromodeoxyuridine–labeled monocytes/macrophages in the fatty streak and resulted in reduced lesion size in *Ldlr*^{-/-} mice fed a high fat diet for 2 weeks. In vitro studies to investigate the mechanisms involved revealed that macrophages from *Ddr1*^{-/-} mice had decreased adhesion to type IV collagen and decreased chemotactic invasion of type IV collagen in response to monocyte chemoattractant protein-1.

Conclusions: Taken together, our data support an independent and critical role for DDR1 in macrophage accumulation at early and late stages of atherogenesis. (*Circ Res.* 2009;105:1141-1148.)

Key Words: atherosclerosis ■ discoidin domain receptor ■ collagen ■ macrophage ■ inflammation

The accumulation of macrophages in the arterial intima is a critical event in atherosclerotic plaque development. Macrophage accumulation depends on a series of well-defined interactions with the endothelium, culminating in transmigration and invasion of the subendothelial extracellular matrix.¹ In the atherosclerotic intima, monocytes/macrophages interact with an extracellular matrix rich in several types of collagen. Collagens are important components of the extracellular matrix present within atherosclerotic plaques: contributing to lesion volume, enhancing the mechanical stability of the fibrous cap, and providing key signals that regulate monocyte differentiation, protease expression, and the production of inflammatory mediators.²

The discoidin domain receptors (DDRs) are a subfamily of receptor tyrosine kinases that transduce signals when bound

to collagens. There are 2 *Ddr* genes in the human and mouse genomes, *Ddr1* and *Ddr2*,³ and 6 differentially spliced isoforms of DDR1 have been identified (termed *Ddr1a-e*, and an isoform only expressed in rat testes).^{4,5} Both DDR1 and DDR2 bind to several collagen subtypes, but the receptors require an intact triple helical domain for signaling; denatured collagen, or gelatin, does not induce signaling through DDrs.^{6–8} Importantly, DDR1 has been shown to signal when bound to collagen types I to V and VIII, a ligand repertoire that includes fibril forming interstitial collagens (types I to III), as well as network-forming type IV collagen, a principal component of the endothelial basement membrane.

Ferri et al have reported the expression of DDR1 in the atherosclerotic plaques of nonhuman primates.⁹ We have recently identified a functional role for DDR1 in the regula-

Original received August 27, 2008; resubmission received August 14, 2009; revised resubmission received September 28, 2009; accepted October 2, 2009.

From the Department of Laboratory Medicine and Pathobiology, University of Toronto, Ontario, Canada.

Correspondence to Dr Michelle Bendeck, PhD, Department of Laboratory Medicine and Pathobiology, University of Toronto, Medical Sciences Building, Room 6213, 1 King's College Circle, Toronto, ON M5S 1A8, Canada. E-mail michelle.bendeck@utoronto.ca

© 2009 American Heart Association, Inc.

Circulation Research is available at <http://circres.ahajournals.org>

DOI: 10.1161/CIRCRESAHA.109.207357

Non-standard Abbreviations and Acronyms

BrdUrd	5-bromodeoxyuridine
DDR	discoidin domain receptor
FITC	fluorescein isothiocyanate
LDLR	low-density lipoprotein receptor
MMP	matrix metalloproteinase
SMC	smooth muscle cell

tion of atherosclerotic plaque inflammation and fibrosis using *Ldlr*^{-/-} mice fed a high-fat diet.¹⁰ Deletion of DDR1 resulted in smaller atherosclerotic plaques that were matrix rich and macrophage poor, both key features of a stable plaque. Accelerated matrix accumulation in *Ddr1*^{-/-}; *Ldlr*^{-/-} plaques resulted from enhanced expression of collagens and elastin by *Ddr1*^{-/-} smooth muscle cells (SMCs) and was associated with decreased in situ matrix metalloproteinase (MMP) activity, as well as reduced lesional macrophage content. However, because DDR1 is expressed both on vessel wall-derived cells such as SMCs and on bone marrow-derived cells such as macrophages, the relative contribution of DDR1 expressed solely by macrophages to plaque development remained unresolved.

In the present study, we have used sex-mismatched bone marrow transplantation to study the role of DDR1 expressed on bone marrow-derived cells such as monocytes/macrophages during atherogenesis. Atherosclerotic plaques from chimeric mice with DDR1-deficient bone marrow (*Ddr1*^{-/-}→^{+/+}) were smaller in size and exhibited reduced accumulation of bone marrow-derived macrophages. Bromodeoxyuridine (BrdUrd) pulse-labeling experiments performed in *Ddr1*^{+/+}; *Ldlr*^{-/-} and *Ddr1*^{-/-}; *Ldlr*^{-/-} mice fed an atherogenic diet for 2 weeks revealed a novel role for DDR1 in macrophage accumulation in the early fatty streak. The mechanisms behind this were revealed by in vitro experiments showing that macrophages from *Ddr1*^{-/-}; *Ldlr*^{-/-} mice exhibited decreased attachment to and invasion of type IV collagen matrix. Our data support an independent role for macrophage DDR1 in atherogenesis and suggest that DDR1 promotes macrophage accumulation and lesion growth by regulating invasion of the intimal basement membrane.

Methods

An expanded Methods section can be found in the Online Data Supplement at <http://circres.ahajournals.org>.

Reciprocal Bone Marrow Transplantation, Analysis of Atherosclerosis, and Histomorphometry

Animal experiments were performed in accordance with the guidelines of the Canada Council on Animal Care. Sex-mismatched bone marrow transplantation was performed using *Ddr1*^{-/-}; *Ldlr*^{-/-} mice and their *Ddr1*^{+/+}; *Ldlr*^{-/-} littermates.¹⁰ The experimental groups included female *Ddr1*^{+/+}; *Ldlr*^{-/-} hosts receiving male *Ddr1*^{+/+}; *Ldlr*^{-/-} bone marrow (*Ddr1*^{+/+}→^{+/+}; control), and female *Ddr1*^{+/+}; *Ldlr*^{-/-} hosts receiving male *Ddr1*^{-/-}; *Ldlr*^{-/-} bone marrow (*Ddr1*^{-/-}→^{+/+}; bone marrow deletion). Three weeks after transplantation, mice were placed on an athero-

genic diet containing 40% kcal of fat and 1.25% cholesterol by weight (Research Diets, D12108) for 12 weeks. After 12 weeks, mice were euthanized by anesthetic overdose and the heart, kidneys, and descending aorta (downstream of the left subclavian artery to the iliac bifurcation) were fixed in 4% paraformaldehyde. The aortic sinus was embedded in paraffin and sectioned into 5- μ m-thick cross-sections. Details of the methods used for analysis of male:female chimerism can be found in the Online Data Supplement. Plasma lipid analysis, oil red O staining of the descending aorta, Verhoeff's van Gieson, picosirius red and LC-PolScope analysis of fibrillar collagen were performed as described previously, and additional details can be found in the online supplement.¹⁰

Y Chromosome Fluorescence In Situ Hybridization and Analysis of Plaque Cellular Content

After deparaffinization in xylenes, air-dried cross-sections of the aortic sinus were denatured in 10 mmol/L sodium citrate (pH 6.0) for 2 hours at 80°C, rinsed in 2 \times sodium chloride/sodium citrate buffer (SSC), and digested in Pepsin (0.22 mg/mL) in 0.1 mol/L HCl for 2 hours at 37°C. Dehydrated sections were then incubated with 3.3 μ L of CY3-labeled mouse Y chromosome Paint probe (Cambio), cover-slipped, and sealed with rubber cement before overnight hybridization at 37°C. After posthybridization washes in 0.1 \times SSC/0.3% NP-40 at 75°C for 3 minutes and 4 \times SSC/0.1% NP-40 for 10 minutes, slides were counterstained with Hoechst 33528 (1:10 000 in distilled water). Y chromosome-positive cells were counted using a Zeiss Axioplan epifluorescence microscope with a \times 100 oil immersion lens.

To determine the relative contribution of vessel wall (ie, host) and bone marrow (ie, donor)-derived cells to lesion, the number of Y chromosome-positive cells was subtracted from the total number of nuclei in the plaque. The difference reflects the number of resident vessel wall-derived cells, for example SMCs, in the lesion.

BrdUrd Pulse Labeling and Measurement of Fatty Streak Lesion Size

Macrophage accumulation into the fatty streak was assessed by BrdUrd pulse labeling.^{11,12} *Ddr1*^{+/+}; *Ldlr*^{-/-} and *Ddr1*^{-/-}; *Ldlr*^{-/-} mice were fed the atherogenic diet for 2 weeks, then given a single IV injection of BrdUrd (10 mg/mL, 0.2 mL volume) to label a cohort of proliferating cells in both the bone marrow and aortic intima at the time of the injection. Mice were euthanized 2 or 24 hours later, and the ascending aorta (aortic sinus to brachiocephalic artery) was whole mount immunostained for BrdUrd using fluorescein isothiocyanate (FITC)-tyramide amplification (Tyramide signal amplification; Perkin Elmer) and mounted en face. Costaining of nuclei and lipids was performed using Hoescht 33528 (1:10 000 in distilled H₂O) and oil red O, respectively.

The total number of BrdUrd-positive cells in the ascending aorta was counted using an Olympus Fluoview confocal microscope with a \times 60 oil immersion lens. As previously reported, BrdUrd-positive cells cannot be detected in the circulation at 2 hours¹¹; therefore, the number of BrdUrd-positive cells in the aortic intima at 2 hours provides a baseline measurement of intimal macrophage proliferation. In contrast, between 6 and 24 hours, there is a detectable cohort of BrdUrd-positive monocytes present in the circulation.¹¹ Therefore, an increase in the BrdUrd-positive cell number in the aortic intima between 2 and 24 hours reflects the accumulation of newly labeled monocytes/macrophages in the developing fatty streak by a combination of local proliferation and recruitment from the circulation over a 22 hour time period. The number of BrdUrd-positive cells per ascending aorta at each time point is expressed per unit of fatty streak lesion surface area to account for differences in lesion size between groups.

Measurement of fatty streak lesion size was carried out using oil red O fluorescence and confocal microscopy as detailed in the online supplement. Low magnification images of the en face preparations of ascending aorta were captured using a Bio-Rad confocal microscope with a \times 4 objective. Measurement of the percentage of aortic surface

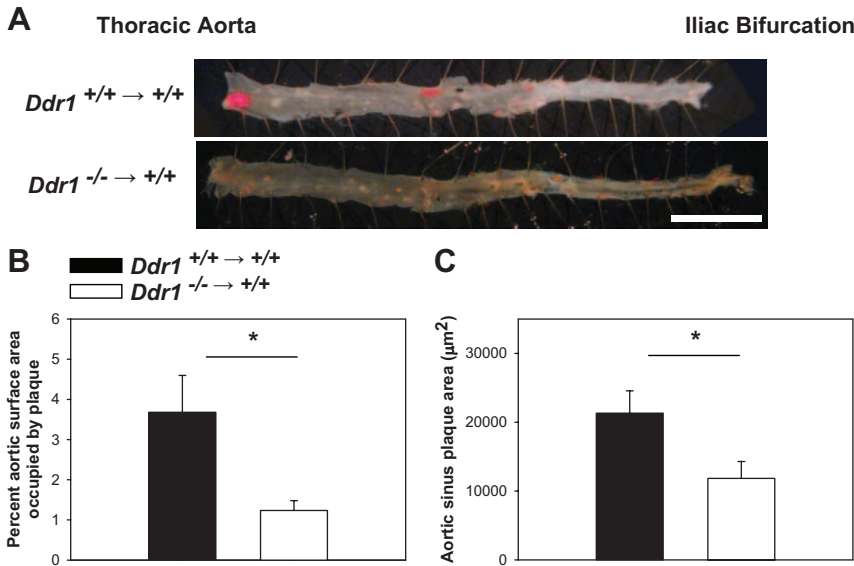


Figure 1. Deletion of DDR1 in bone marrow–derived cells attenuated atherogenesis. **A**, Images of en face preparations of the descending aorta from *Ddr1*^{+/+→+/+} and *Ddr1*^{-/-→+/+} mice, stained with oil red O to label the plaques. **B**, Quantification of atherosclerotic plaque burden expressed as the percentage of aortic surface area occupied by plaque. **C**, Quantification of plaque area on cross-sections from the aortic sinus of chimeric mice. **P*<0.05, significant difference between genotypes (n=7 animals per group). Scale bar=5 mm.

area occupied by plaque was carried out using Simple PCI quantitative imaging software.

Flow Cytometry

Ddr1^{+/+;Ldlr}^{-/-} or *Ddr1*^{-/-;Ldlr}^{-/-} mice fed the atherogenic diet for 2 weeks were pulse labeled with BrdUrd for 24 hours, and samples of peripheral blood (100 μL) or bone marrow (10⁶ cells) were taken to measure intracellular staining of BrdUrd using flow cytometry (FITC-BrdUrd flow kit, Becton Dickinson) according to the instructions of the manufacturer. Costaining for monocytes in peripheral blood was performed using the following markers: CD115-phycoerythrin (1:100, eBioscience), Ly-6C-biotin (1:200, BMA), and streptavidin-allophycocyanin (SA-APC, 1:800, Becton-Dickinson). Samples were analyzed on a Beckman Coulter FC500 flow cytometer at the following wavelengths: FITC: 510 nm/540 nm, phycoerythrin: 560 nm/590 nm; APC: 660 nm/690 nm.

Statistical Analysis

Data are presented as means±SEM. All statistical analysis was carried out using Sigma Stat (SyStat Software Inc). Pairwise comparisons between transplant groups or genotypes were performed using Student’s *t* test. Data that did not fit a normal distribution were analyzed by Mann–Whitney *U* test for nonparametric comparisons. BrdUrd pulse data were analyzed using a 1-way ANOVA with a Tukey post hoc analysis for pairwise comparisons. Statistical significance was determined at *P*<0.05.

Results

Bone Marrow Transplantation, Assessment of Sry Chimerism, and Plasma Lipids

Body weight and fasting plasma cholesterol and triglycerides measured after 12 weeks on the atherogenic diet (15 weeks after transplant) were comparable between transplant groups (Online Table I). Male:female chimerism measured after 12 weeks on the atherogenic diet was assessed by analyzing genomic DNA isolated from peripheral blood leukocytes for *Ddr1* and *Sry*, a marker of the Y chromosome (Online Figure I, A). Leukocyte DNA from *Ddr1*^{-/-→+/+} mice demonstrated the presence of the donor genotype (*Ddr1*^{-/-}), with negligible host DNA remaining. (Online Figure I, A, top). The abundance of leukocyte *Sry* was comparable in all chimeric mice (Online Figure I, A, bottom), and this was

confirmed by measuring the ratio of *Sry/Gapdh* by quantitative real-time PCR (Online Figure I, B).

DDR1 Expressed on Bone Marrow–Derived Cells Promotes Atherogenesis

Deletion of *Ddr1* in bone marrow–derived cells (*Ddr1*^{-/-→+/+}) resulted in a marked reduction in atherosclerotic plaque burden in the descending aorta compared to *Ddr1*^{+/+→+/+} mice (Figure 1A). Quantification of the percentage aortic surface area occupied by oil red O–positive plaque revealed a significant 66% decrease in atherosclerotic plaque burden in *Ddr1*^{-/-→+/+} mice compared to *Ddr1*^{+/+→+/+} mice (Figure 1B). Furthermore, atherosclerotic plaque area measured in cross-sections of the aortic sinus was reduced by 44% in *Ddr1*^{-/-→+/+} mice compared to *Ddr1*^{+/+→+/+} mice (Figure 1C). Taken together, these data confirm a critical role for DDR1 expressed on bone marrow–derived cells in atherosclerotic plaque growth and development.

Bone Marrow–Derived Macrophage Accumulation Was Reduced in *Ddr1*^{-/-→+/+} Plaques

Because male bone marrow donors were used to generate the chimeric mice, we were able to detect bone marrow–derived cells in the lesions using fluorescence in situ hybridization for the Y chromosome. Y chromosome–positive cells were abundant within the plaque and were also observed in the adventitia but were not observed in the media (Figure 2A and 2B). Correlative immunofluorescence staining with antibodies against Mac-2, smooth muscle α-actin, or vascular cell adhesion molecule-1 confirmed that the majority of the lesional Y chromosome–positive cells were macrophages (Online Figure II and data not shown). Quantification of the number of Y chromosome–positive cells in the plaques revealed a significant 47% decrease in bone marrow–derived macrophage accumulation in *Ddr1*^{-/-→+/+} mice compared to *Ddr1*^{+/+→+/+} mice (Figure 2C, gray bars). Furthermore, the decrease in bone marrow–derived macrophages was responsible for the decrease in total cell number that was observed in the aortic sinus lesions of *Ddr1*^{-/-→+/+} mice

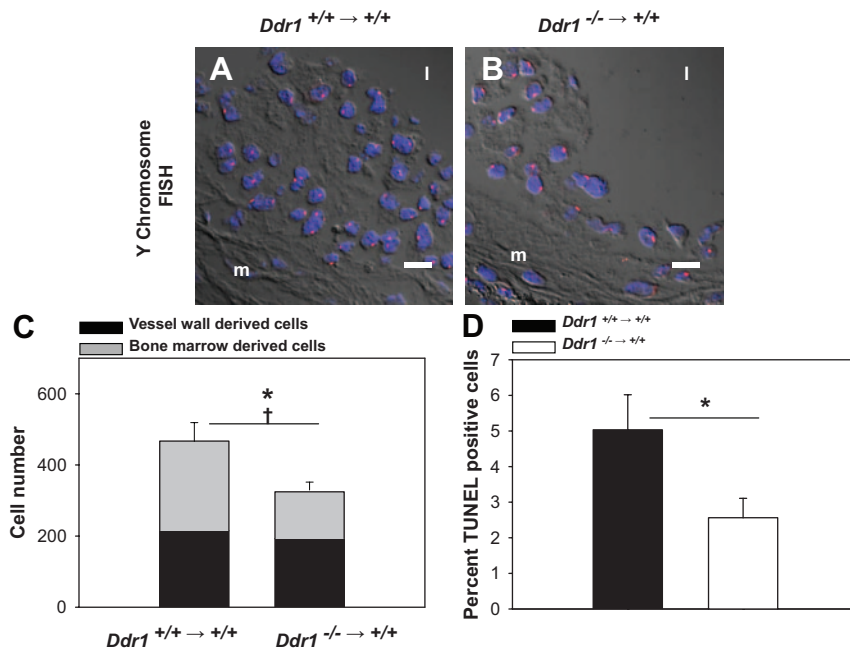


Figure 2. Accumulation of bone marrow–derived cells was reduced in the plaques from *Ddr1*^{-/-}→^{+/+} mice. A and B, Confocal images of Y chromosome–positive cells in macrophage rich regions of atherosclerotic plaques from the aortic sinus of *Ddr1*^{+/+}→^{+/+} (A) and *Ddr1*^{-/-}→^{+/+} mice (B). Nuclei are stained blue; the Y chromosome Paint probe is red, and a differential interference contrast image was overlaid to highlight lesion morphology. m indicates media, l indicates lumen. C, Quantification of the number of Y chromosome–positive, bone marrow–derived cells in the lesions of chimeric mice (gray bars), the number of resident vessel wall–derived cells (black bars), and the total plaque cell number (sum of gray bars and black bars). **P*<0.05, significant difference in Y chromosome–positive cell number between genotypes; †*P*<0.05, significant difference in total cell number between genotypes. (n=6 animals per group). Scale bar=10 μm. D, Quantification of the percentage of TUNEL–positive nuclei in atherosclerotic plaques of *Ddr1*^{+/+}→^{+/+} and *Ddr1*^{-/-}→^{+/+} mice. **P*<0.05, significant difference in the percentage of TUNEL–positive cells.

compared to *Ddr1*^{+/+}→^{+/+} mice (467±53 versus 324±24; Figure 2C, sum of black and gray bars). In contrast, bone marrow–specific deletion of DDR1 had no effect on the number of host–derived resident vessel wall cells (Figure 2C, black bars). Taken together with the reduction in lesion size, these data suggest that deficiency of DDR1 in bone marrow–derived cells specifically limits the accumulation of macrophages in the developing plaques, which results in the attenuation of lesion growth.

The net accumulation of macrophages in the atherosclerotic plaque is influenced by macrophage infiltration into the lesion and cell death within the lesion. To determine whether the reduction in macrophage number in *Ddr1*^{-/-}→^{+/+} plaques was caused by an increase in cell death, we measured the percentage of apoptotic cells in sections of the aortic sinus using TUNEL. The percentage of TUNEL–labeled cells was significantly decreased in *Ddr1*^{-/-}→^{+/+} mice compared to *Ddr1*^{+/+}→^{+/+} mice (Figure 2D). Therefore, these data are consistent with the hypothesis that the reduction in plaque macrophages observed in *Ddr1*^{-/-}→^{+/+} mice was the result of impaired infiltration into the lesion and not attributable to increased cell death.

Matrix Composition Was Similar in *Ddr1*^{-/-}→^{+/+} and *Ddr1*^{+/+}→^{+/+} Plaques

To evaluate changes in matrix composition of the atherosclerotic plaques from *Ddr1*^{+/+}→^{+/+} and *Ddr1*^{-/-}→^{+/+} mice, we stained serial sections of aortic sinus with Verhoeff's van Gieson and picrosirius red to identify elastin and collagen respectively (Figure 3). Despite the significant reduction in plaque size, measurement of the percentage of lesion area occupied by collagen or elastin demonstrated no difference between groups. Similarly, using the LC–PolScope, which detects the retardance of polarized light by fibrillar collagens, we observed comparable fibrillar collagen content of plaques between transplant groups (Figure 3).

Deficiency of DDR1 Limits the Infiltration of BrdUrd–Labeled Monocytes/Macrophages in the Developing Fatty Streak

Because our findings on well–developed atherosclerotic plaques indicated reduced macrophage accumulation in the *Ddr1*^{-/-}→^{+/+} lesions that could be attributed to decreased macrophage infiltration, we wished to determine whether this deficit was also present at the earliest stages of lesion development: the formation of the fatty streak. The fatty streak provides a simplified in vivo model to study the role of DDR1 in macrophage infiltration because the majority of lesional cells are macrophage foam cells and there is little SMC involvement or lesion fibrosis. We performed BrdUrd pulse labeling in *Ddr1*^{+/+}; *Ldlr*^{-/-} and *Ddr1*^{-/-}; *Ldlr*^{-/-} mice fed an atherogenic diet for 2 weeks. Mice were given a single pulse injection of BrdUrd, which labeled a cohort of proliferating cells in the bone marrow and allowed us to track their subsequent infiltration and accumulation in the atherosclerotic intima using en face confocal microscopy.

Fasting plasma lipids assayed after 2 weeks on the atherogenic diet were comparable between the two genotypes (Online Table II), and the proportion of BrdUrd–positive monocytes in the circulation and the bone marrow were also similar between groups (Figure 4A and 4B). Measurement of the percentage of ascending aortic surface area occupied by fatty streak was carried out by en face confocal imaging, which revealed a significant decrease in lesion size in *Ddr1*^{-/-}; *Ldlr*^{-/-} mice compared to *Ddr1*^{+/+}; *Ldlr*^{-/-} mice (Figure 4C). These data provide the first evidence of a role for DDR1 as a regulator of fatty streak formation. Independent of the change in lesion size, the deficiency of DDR1 also limited the infiltration of BrdUrd labeled monocytes/macrophages into the fatty streak. Figure 5A and 5B show the extent of oil red O–stained fatty streak, and Figure 5C and 5D show the BrdUrd–labeled cells in the lesions. *Ddr1*^{+/+}; *Ldlr*^{-/-} mice exhibited a significant increase in the number of BrdUrd⁺

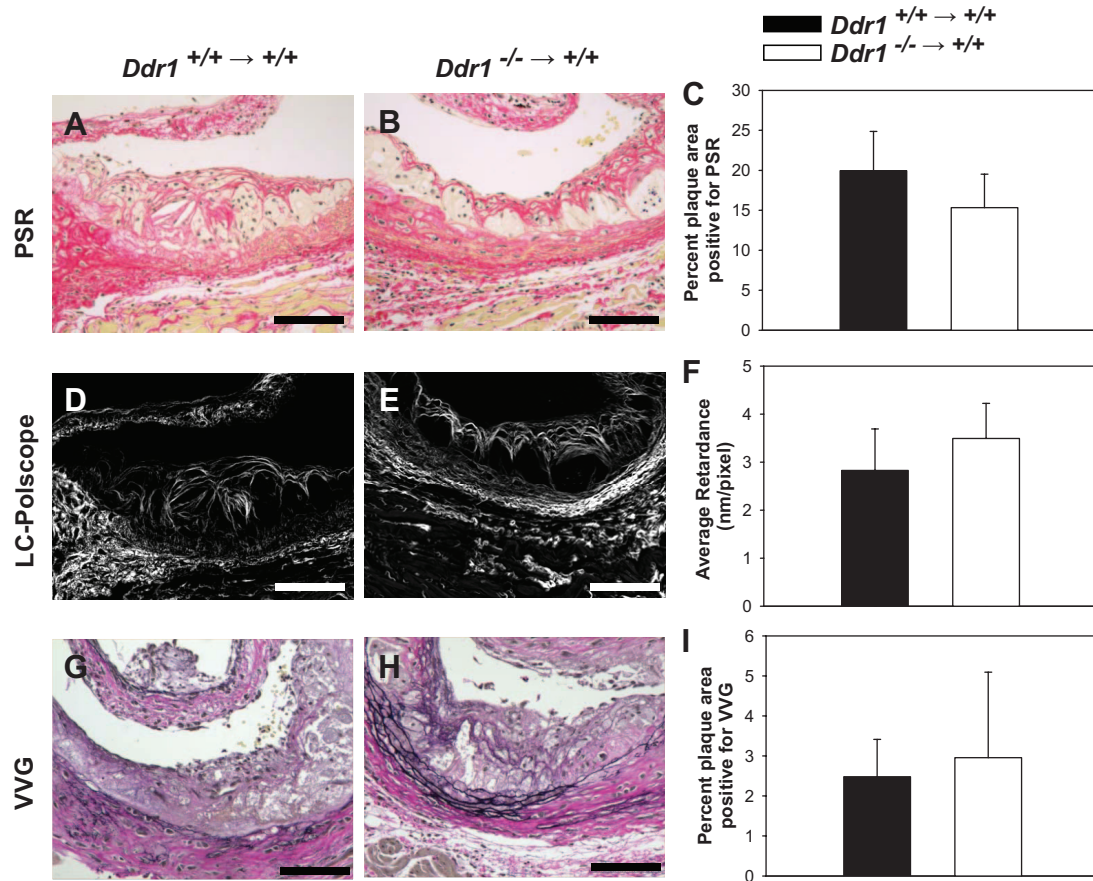


Figure 3. Similar matrix composition of atherosclerotic plaques from *Ddr1*^{-/-}→*+/+* and *Ddr1*^{+/-}→*+/+* mice. A, B, D, and E, Light microscopic images (A and B) and corresponding PolScope images (D and E) of picosirius red stained cross-sections from the aortic sinus of chimeric mice to detect collagen. C and F, Quantification of the percentage plaque area positive for picosirius red staining on light microscopic images (C) or the average birefringence retardance of fibrillar collagen measured by LC-PolScope (F). G and H, Light micrographs of cross-sections from the aortic sinus from chimeric mice stained with Verhoeff's van Gieson to detect elastin. I, Quantification of the percentage of plaque area that stained positive for elastin (n=7 animals per group). Scale bar=100 μm.

cells per unit of lesion area between 2 and 24 hours (Figure 5E), indicating that an accumulation of labeled macrophages occurred during this time period. By contrast, the number of BrdUrd⁺ cells per unit of lesion area in the *Ddr1*^{-/-};*Ldlr*^{-/-} mice was unchanged between 2 and 24 hours (Figure 5E). Taken together, these data suggest that macrophage infiltration in the fatty streak was impaired in *Ddr1*^{-/-};*Ldlr*^{-/-} mice, which resulted in reduced fatty streak lesion size.

To determine whether the attenuation of macrophage infiltration in DDR1-deficient animals also occurred in response to a general inflammatory stimulus, we measured macrophage accumulation in the peritoneum after an injection of thioglycollate. The percentage of macrophages in the peritoneal lavage was 12.3±2.3% in *Ddr1*^{-/-};*Ldlr*^{-/-} mice compared to 15.5±1% in *Ddr1*^{+/-};*Ldlr*^{-/-} mice; however, the difference was not statistically significant.

DDR1 Regulates Macrophage Infiltration by Promoting the Interaction With and Invasion of Type IV Collagen Matrices

Emerging evidence supports a role for DDR1 as a mediator of matrix invasion in multiple cell types.² Therefore, to further investigate the mechanisms behind the reduction in macrophage accumulation, we assayed the adhesion and invasion of perito-

neal macrophages from *Ddr1*^{+/-};*Ldlr*^{-/-} and *Ddr1*^{-/-};*Ldlr*^{-/-} mice through type IV collagen matrices in vitro. Type IV collagen is a principal component of the endothelial basement membrane and likely the first collagenous barrier to be encountered by a macrophage invading the plaque. Adhesion of *Ddr1*^{-/-} macrophages to type IV collagen was significantly reduced by 51% compared to *Ddr1*^{+/-} cells (Figure 6A). Next, we assayed the monocyte chemoattractant protein-1-dependant chemotaxis of *Ddr1*^{+/-} or *Ddr1*^{-/-} peritoneal macrophages through type IV collagen and found that *Ddr1*^{-/-} macrophages exhibited a 50% reduction in chemotactic invasion through type IV collagen compared to *Ddr1*^{+/-} macrophages (Figure 6B). These data suggest that deficiency of DDR1 limits the ability of macrophages to adhere to and invade through collagen matrix barriers, key steps in their infiltration and accumulation in the arterial intima.

Discussion

Using a bone marrow transplantation approach, we have identified an independent role for DDR1 expressed on macrophages in contributing to atherosclerotic plaque development by regulating macrophage infiltration and accumulation in the plaque. The reduction in lesion size and cellularity in

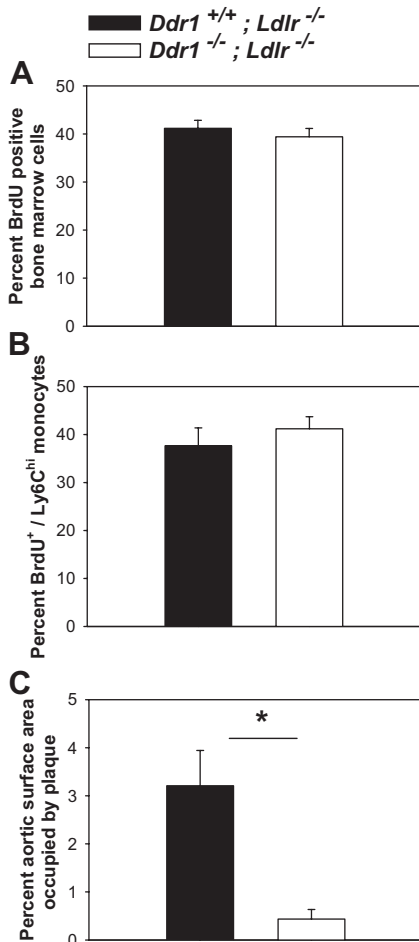


Figure 4. BrdUrd labeling of bone marrow and circulating monocytes is comparable in *Ddr1*^{-/-};*Ldlr*^{-/-} and *Ddr1*^{+/+};*Ldlr*^{-/-} mice. A and B, The percentage of BrdUrd-positive bone marrow cells (A) and circulating CD115⁺/Ly6C^{hi} monocytes (B) was determined by flow cytometry (n=4 animals per group). C, DDR1 deficiency attenuates fatty streak formation. Quantification of the percentage of aortic surface area occupied by oil red O-positive fatty streak. *P<0.05, significant difference between genotypes (n=12 to 13 animals per group).

Ddr1^{-/-→+/+} mice was attributable to decreased bone marrow-derived macrophage accumulation and was associated with impaired adhesion and invasion through type IV collagen matrices by *Ddr1*^{-/-} macrophages. Furthermore, we have determined that DDR1-dependant macrophage accumulation is also critical for the formation of the fatty streak, one of the earliest stages of lesion development. Taken together, our data suggest that DDR1 expression on macrophages, by facilitating the interaction with and invasion through type IV collagen-rich matrices such as the endothelial basement membrane, mediates macrophage accumulation and contributes to lesion growth at multiple stages.

We show that deletion of DDR1 on bone marrow-derived macrophages is sufficient to result in decreased plaque growth at both early (2 weeks) and late (12 weeks) stages of plaque development. That the reduction in plaque size is a consequence of reduced macrophage accumulation is evidenced by comparing the specific decrease in donor-derived macrophage cell number (47% decrease), and the parallel and

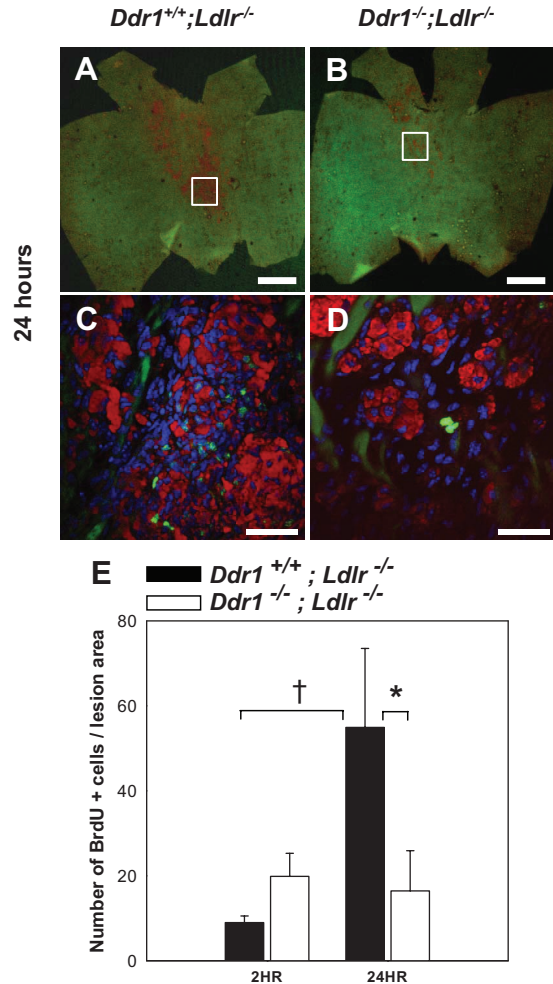


Figure 5. DDR1 deficiency attenuates macrophage accumulation during early atherogenesis. A and B, En face epifluorescence images of the ascending aorta of *Ddr1*^{+/+};*Ldlr*^{-/-} and *Ddr1*^{-/-};*Ldlr*^{-/-} mice after 2 weeks on the atherogenic diet to demonstrate the size and distribution of the fatty streak lesions. Red indicates oil red O-positive lipid; green, internal elastic lamina autofluorescence. Boxes indicate areas that were scanned at high magnification using confocal microscopy to acquire the images in C and D. Scale bar=1 mm. C and D, Confocal images showing BrdUrd-positive cells in atherosclerotic plaques from the ascending aorta of *Ddr1*^{+/+};*Ldlr*^{-/-} and *Ddr1*^{-/-};*Ldlr*^{-/-} mice 24 hours after BrdUrd pulse injection. Bright green indicates BrdUrd-positive cells; darker green, internal elastic lamina autofluorescence; blue, nuclei; red, oil red O-positive lipid. Scale bar=50 μm. E, Quantification of the number of BrdUrd-positive cells per unit of lesion area in the ascending aorta at 2 or 24 hours after the BrdUrd injection. *P<0.05, significant difference between genotypes at 24 hours; †P<0.05, significant difference between *Ddr1*^{+/+};*Ldlr*^{-/-} mice at 2 and 24 hours after injection (n=4 to 6 animals per group).

equivalent reduction in plaque size (44% decrease). Furthermore, even at the earliest stages of plaque development, deficiency of DDR1 limits the infiltration of BrdUrd-labeled monocytes/macrophages into the lesion. By allowing us to dissect out the relative role of DDR1 on macrophages versus SMCs in plaque growth, these novel findings expand on our previous work examining the effects of systemic deletion of DDR1 during atherogenesis¹⁰ and point to an important and independent role for DDR1 on macrophage infiltration to the atherosclerotic plaque.

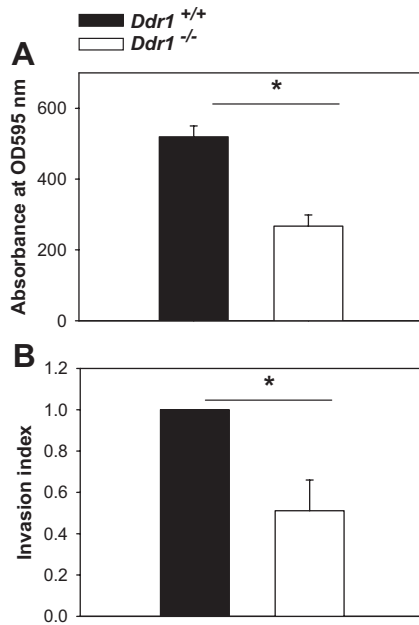


Figure 6. *Ddr1*^{-/-} macrophages exhibit impaired attachment to and chemotactic invasion through a type IV collagen matrix. **A**, Peritoneal macrophages from *Ddr1*^{+/+}; *Ldlr*^{-/-} or *Ddr1*^{-/-}; *Ldlr*^{-/-} mice were allowed to adhere for 2 hours to plates coated with type IV collagen, and the number of adherent cells was assessed by staining with toluidine blue dye and measuring absorbance at 595 nm. **B**, Macrophages were allowed to invade type IV collagen-coated transwell chambers in response to monocyte chemoattractant protein-1. The invasion index is the fold increase in collagen invasion response to monocyte chemoattractant protein-1 compared to serum free medium, and data are expressed relative to *Ddr1*^{+/+} macrophages. Each experiment was repeated 3 times. *Significant difference between groups.

Another very important finding in our present study is the discovery that there is a reduction in fatty streak lesion size in *Ddr1*^{-/-}; *Ldlr*^{-/-} mice, which provides the first evidence of a role for DDR1 in one of the earliest stages of atherogenesis. Moreover, these data are consistent with our previous work showing attenuation of much more advanced lesions in both the *Ddr1*^{-/-}; *Ldlr*^{-/-} mice at 12 and 24 weeks¹⁰ and in the *Ddr1*^{-/-}→^{+/+} chimeras at 12 weeks (present study). Taken together, our data support the notion that deficiency of DDR1 in macrophages early in atherogenesis may have long-term consequences for disease progression at later time points and underscores the importance of DDR1 as a potential target in the long-term management of atherosclerotic disease.

These results prompted us to investigate the mechanisms whereby DDR1 promotes macrophage infiltration and accumulation within the plaque. Because DDR1 is a collagen receptor, it was logical to hypothesize that newly recruited monocytes would use DDR1 to adhere to and traverse the collagen-rich plaque matrix. Indeed, we found that DDR1-deficient macrophages exhibited a reduced capacity to interact with and traverse a type IV collagen matrix. It is likely that the failure of macrophages to traverse the matrix is related to the attenuation of MMP production, because we have shown that MMP expression is reduced in *Ddr1*^{-/-} macrophages,¹⁰ and others have reported that DDR1 overexpression in a macrophage cell line enhanced type I collagen

matrix invasion.¹³ Furthermore, collagen signaling has been shown to regulate the production of MMP-1 and MMP-9 in human macrophages.^{14–16} These data strongly suggest that the regulation of MMP expression is the mechanism for DDR1-mediated matrix invasion. Taken together, these findings suggest that DDR1 deficiency in macrophages limits macrophage invasion of the endothelial basement membrane and plaque extracellular matrix.

To assess whether DDR1 deficiency also limited macrophage infiltration to a more general inflammatory stimulus, we assayed peritoneal macrophage accumulation after an injection of thioglycollate. We observed a trend toward a reduction in peritoneal macrophage accumulation in DDR1-deficient mice; however, the reduction was not statistically significant and was not as great as we observed in the atherosclerotic plaque. Recently, Voisin et al demonstrated that monocytes preferentially traverse the basement membrane of postcapillary venules at sites of low matrix protein expression, termed low expression regions (LERs). Moreover, their data suggest that monocyte transmigration at LERs does not require proteases.¹⁷ Because LERs have not been demonstrated in the matrix rich subendothelial basement membrane of the aortic intima, it is possible that protease dependant transmigration at this arterial location could account for the differences observed between macrophage infiltration in atherosclerotic plaques versus peritoneal inflammation.

Despite the dramatic change in plaque size and cell accumulation, the atherosclerotic plaques from *Ddr1*^{-/-}→^{+/+} chimeric mice exhibited no difference in the proportion of lesion area occupied by matrix molecules compared to *Ddr1*^{+/+}→^{+/+} controls. By contrast, in previous work examining the advanced plaques of *Ddr1*^{-/-}; *Ldlr*^{-/-} mice (with systemic deletion of DDR1), we observed an acceleration of collagen and elastin deposition and increased fibrosis compared to *Ddr1*^{+/+}; *Ldlr*^{-/-} mice, and we also documented increased collagen and elastin expression by DDR1-deficient SMCs in vitro.¹⁰ This suggests that enhanced matrix accumulation is the result of DDR1 deletion in SMCs alone, and that macrophage DDR1 deficiency does not contribute to the enhanced matrix accumulation observed in the lesions of *Ddr1*^{-/-}; *Ldlr*^{-/-} mice.

Emerging evidence supports a role for DDR1 in leukocyte accumulation in chronic inflammatory diseases such as renal¹⁸ and pulmonary fibrosis.¹⁹ Using bone marrow transplantation, we demonstrate, for the first time, an independent role for macrophage DDR1 in atherosclerotic plaque development. Our data support a model whereby DDR1 facilitates the invasion and accumulation of monocytes/macrophages in the arterial intima by mediating the interaction with and invasion through the type IV collagen-rich endothelial basement membrane, resulting in reduced macrophage accumulation, decreased intimal inflammation, and the attenuation of atherogenesis.

Acknowledgments

We thank Dr Phillip Connelly and Graham Maguire for assistance with measurements of plasma lipoproteins and triglycerides; Dr Jeremy Squire for advice on the fluorescence in situ hybridization;

and Dr Philip Marsden and Brent Steer for assistance with the real-time PCR.

Sources of Funding

This study was funded by Canadian Institutes of Health Research grant MOP37847 and Heart and Stroke Foundation of Ontario grants NA6069 and T6734 (to M.P.B.). M.P.B. and M.C. are Career Investigators of the Heart and Stroke Foundation of Ontario. C.F. was supported by a Doctoral Research Award from the Heart and Stroke Foundation of Canada, a Canada Graduate Scholarship Doctoral Award from the Canadian Institutes of Health Research, and the Meredith and Malcolm Silver Scholarship in Cardiovascular Studies. K.B. was supported by a Masters Award from the Heart and Stroke Foundation of Ontario. E.W. was supported by a John D. Schultz Scholarship from the Heart and Stroke Foundation of Ontario.

Disclosures

None.

References

- Ley K, Laudanna C, Cybulsky MI, Nourshargh S. Getting to the site of inflammation: the leukocyte adhesion cascade updated. *Nat Rev Immunol.* 2007;7:678–689.
- Adiguzel E, Ahmad PJ, Franco C, Bendeck MP. Collagens in the progression and complications of atherosclerosis. *Vasc Med.* 2009;14:73–89.
- Vogel WF, Abdulhussein R, Ford CE. Sensing extracellular matrix: an update on discoidin domain receptor function. *Cell Signal.* 2006;18:1108–1116.
- Alves F, Saube S, Ledwon M, Schaub F, Hiddemann W, Vogel WF. Identification of two novel, kinase-deficient variants of discoidin domain receptor 1: differential expression in human colon cancer cell lines. *FASEB J.* 2001;15:1321–1323.
- Mullenbach E, Walter L, Dressel R. A novel discoidin domain receptor 1 (Ddr1) transcript is expressed in postmeiotic germ cells of the rat testis depending on the major histocompatibility complex haplotype. *Gene.* 2006;372:53–61.
- Leitinger B, Kwan AP. The discoidin domain receptor DDR2 is a receptor for type X collagen. *Matrix Biol.* 2006;25:355–364.
- Hou G, Vogel W, Bendeck MP. The discoidin domain receptor tyrosine kinase DDR1 in arterial wound repair. *J Clin Invest.* 2001;107:727–735.
- Vogel W, Gish GD, Alves F, Pawson T. The discoidin domain receptor tyrosine kinases are activated by collagen. *Mol Cell.* 1997;1:13–23.
- Ferri N, Carragher NO, Raines EW. Role of discoidin domain receptors 1 and 2 in human smooth muscle cell-mediated collagen remodeling: potential implications in atherosclerosis and lymphangioliomyomatosis. *Am J Pathol.* 2004;164:1575–1585.
- Franco C, Hou G, Ahmad PJ, Fu EYK, Koh L, Vogel WF, Bendeck MP. Discoidin domain receptor 1 (*Ddr1*) deletion decreases atherosclerosis by accelerating matrix accumulation and reducing inflammation in low-density lipoprotein receptor-deficient mice. *Circ Res.* 2008;102:1202–1211.
- Jongstra-Bilen J, Haidari M, Zhu SN, Chen M, Guha D, Cybulsky MI. Low-grade chronic inflammation in regions of the normal mouse arterial intima predisposed to atherosclerosis. *J Exp Med.* 2006;203:2073–2083.
- Kriss JP, Revesz L, Tung L, Eglhoff S. The distribution and fate of bromodeoxyuridine and bromodeoxycytidine in the mouse and rat. *Cancer Res.* 1962;22:254–265.
- Kamohara H, Yamashiro S, Galligan C, Yoshimura T. Discoidin domain receptor 1 isoform-a (DDR1a) promotes migration of leukocytes in three-dimensional collagen lattices. *FASEB J.* 2001;15:2724–2726.
- Shapiro SD, Kobayashi DK, Pentland AP, Welgus HG. Induction of macrophage metalloproteinases by extracellular matrix. Evidence for enzyme- and substrate-specific responses involving prostaglandin-dependent mechanisms. *J Biol Chem.* 1993;268:8170–8175.
- Wesley RB, Meng X, Godin D, Galis ZS. Extracellular matrix modulates macrophage functions characteristic to atheroma: collagen type I enhances acquisition of resident macrophage traits by human peripheral blood monocytes in vitro. *Arterioscler Thromb Vasc Biol.* 1998;18:432–440.
- Lepidi S, Kenagy RD, Raines EW, Chiu ES, Chait A, Ross R, Clowes AW. MMP-9 production by human monocyte-derived macrophages is decreased on polymerized type I collagen. *J Vasc Surg.* 2001;34:1111–1118.
- Voisin MB, Woodfin A, Nourshargh S. Monocytes and neutrophils exhibit both distinct and common mechanisms in penetrating the vascular basement membrane in vivo. *Arterioscler Thromb Vasc Biol.* 2009;29:1193–1199.
- Flamant M, Placier S, Rodenas A, Curat CA, Vogel WF, Chatziantoniou C, Dussaule JC. Discoidin domain receptor 1 null mice are protected against hypertension-induced renal disease. *J Am Soc Nephrol.* 2006;17:3374–3381.
- Avivi-Green C, Singal M, Vogel WF. Discoidin domain receptor 1-deficient mice are resistant to bleomycin-induced lung fibrosis. *Am J Respir Crit Care Med.* 2006;174:420–427.

Expanded Materials & Methods

All materials were purchased from Sigma-Aldrich unless otherwise specified.

Reciprocal bone marrow transplantation and analysis of atherosclerosis.

Animal experiments were performed in accordance with the guidelines of the Canada Council on Animal Care. Sex mismatched bone marrow transplantation was performed using *Ddr1*^{-/-};*Ldlr*^{-/-} mice and their *Ddr1*^{+/+};*Ldlr*^{-/-} littermates.¹ Female *Ddr1*^{+/+};*Ldlr*^{-/-} mice were lethally irradiated (9.5 Gy, Cs-137 source), and reconstituted after 4 hours via tail vein injection with 10 million bone marrow cells isolated from the femurs and tibias of male donor mice. Transplanted mice were housed in sterile cages with sterile food, bedding and water. The experimental groups included female *Ddr1*^{+/+};*Ldlr*^{-/-} hosts receiving male *Ddr1*^{+/+};*Ldlr*^{-/-} bone marrow (*Ddr1*^{+/+} → ^{+/+}: control), and female *Ddr1*^{+/+};*Ldlr*^{-/-} hosts receiving male *Ddr1*^{-/-};*Ldlr*^{-/-} bone marrow (*Ddr1*^{-/-} → ^{+/+}: bone marrow deletion).

Three weeks after transplantation mice were placed on an atherogenic diet containing 40% Kcal fat and 1.25 % cholesterol by weight (Research Diets, D12108) for 12 weeks. After 12 weeks, mice were sacrificed by anesthetic overdose with 67 mg/kg xylazine and 333 mg/kg ketamine i.p. and blood samples were collected for analysis of plasma lipids as previously described.¹ The left ventricle was cannulated and tissues were perfused with 50 ml of sterile saline. The heart, kidneys and descending aorta (downstream of the left subclavian artery to the iliac bifurcation) were fixed in 4 % paraformaldehyde. The descending aorta was used for enface analysis of atherosclerotic plaque burden by oil red o staining as previously described.¹ The aortic sinus was embedded in paraffin and sectioned into 5 um thick cross-sections. Plaque area was measured in Verhoff's van gieson (VVG) stained cross-sections sections using digital image analysis software (Simple PCI). Atherosclerotic plaque present on the aortic valve leaflets was excluded from this analysis.

Assessment of male:female chimerism.

To assess the efficiency of bone marrow reconstitution, genomic DNA was isolated from peripheral blood leukocytes of chimeric mice and quantified by UV absorbance at 260 nm. 45 ng of total DNA was assayed by PCR amplification for *Ddr1* genotype as previously described¹ and using primers for mouse *Sry*, a marker of the Y chromosome (forward: 5'-CGTGGTGAGAGGCACAAGT-3' and reverse: 5'-AACAGGCTGCCAATAAAAGC-3'). PCR reactions for *Sry* were performed as follows: after 2 minutes at 94 °C, the reaction was cycled 35 times at 94 °C for 45 seconds, 58 °C for 45 seconds and at 72 °C for 1 minute.

Male:female chimerism was also assessed by real time PCR using primers for *Sry* and *Gapdh*. Power SYBR Green PCR Master Mix (Applied Biosystems) was used to amplify 9 ng of leukocyte DNA using the 7900HT sequence detection system (Applied Biosystems). Primer sequences used to amplify *Sry* were: forward: 5'-TTATGGTGTGGTCCCGTGGT-3' and reverse: 5'-GGCCTTTTTTCGGCTTCTGT-3'. Primers for *Gapdh* were: forward: 5'-AAGAGAGAGGCCCTATCCCAACTC-3', and reverse: 5'-CCTAGGCCCTCCTGTTATTA-3'. After 10 minutes at 95 °C, the reactions were cycled 40 times at 95 °C for 15 seconds, and then 60 °C for 1 minute. Relative quantification of the ratio of *Sry/Gapdh* in each sample was performed using the formula $2^{-\Delta\Delta C_t}$ and was expressed as a percent relative to the *Ddr1*^{+/+} → ^{+/+} transplant group.

Immunohistochemistry and matrix staining.

Cross sections of the aortic sinus were deparaffinized in xylenes, and rehydrated in an ethanol series. Sections were stained using antibodies against SM α -actin (1:400, Sigma), Mac-2 (1:100, Cedarlane). Sections were incubated with species appropriate biotinylated secondary antibodies followed by incubation with avidin-biotin-HRP complex (ABC elite, Vector Laboratories). Sections were incubated with the chromogenic substrate 3,3'-diaminobenzidine (DAKO Corp), followed by counterstaining with hematoxylin (1:50). For immunofluorescent detection of Mac-2 or SM α -actin, species appropriate, Cy3-conjugated secondary antibodies were used and nuclei were visualized with Hoescht 33528 (1:10000 in dH₂O). Negative controls were performed by omitting the primary antibody. Additional serial sections were stained with picrosirius red (PSR) or Verhoff's van Geison (VVG) for collagen or elastin, respectively. Fibrillar collagen content of lesions was assessed using the LC Polscope, as previously described.¹ The percentage of positively stained plaque area was assessed by colour thresholding of maximum and minimum signals (Simple PCI, C-Imaging).

Y chromosome fluorescence in situ hybridization (FISH) and analysis of plaque cellular content.

Cross sections of the aortic sinus were deparaffinized in xylenes, washed in ethanol and air dried, before incubation in 10mM sodium citrate pH 6.0 for 2 hours at 80°C. Sections were then rinsed in 2X sodium chloride-sodium citrate buffer (SSC) then digested in Pepsin (0.22 mg/ml) in 0.1M HCl for 2 hours at 37°C. After washing in distilled water, sections were dehydrated through an ethanol series and incubated with 3.3 ul of CY3-labelled mouse Y chromosome Paint probe (Cambio), according to the manufacturer's instructions. Sections were coverslipped with 12mm round coverslips and sealed with rubber cement. Sections and probe were denatured at 78 °C for 10 minutes, followed by hybridization for 22 hours in a humidified chamber at 37 °C. After hybridization, the rubber cement was removed and slides were washed in 0.1X SSC/0.3% NP-40 at 75°C for 3 minutes followed by a wash in 4X SSC/0.1% NP-40 for 10 minutes. Slides were then rinsed in 1X SSC and sections were counter-stained with Hoechst 33528 (diluted 1:10000 in distilled water) for 10 minutes, washed in distilled water and coverslipped with Prolong Gold Antifade solution (Molecular Probes). Y chromosome positive cells were counted using a Zeiss Axioplan epifluorescence microscope with a 100X oil immersion lens. Representative images of FISH positive cells were obtained using an Olympus Fluoview confocal microscope with a 60X objective and 2.2X zoom at the following excitation/emission wavelengths: CY3: 543 nm excitation / 567 nm emission, Hoechst: 405nm excitation / 461 nm emission. A DIC image overlay was also captured to allow visualization of tissue morphology.

Analysis of the cellular composition of the lesions was carried out using cell counts. To determine the relative contribution of vessel wall (i.e. host) and bone marrow (i.e. donor) derived cells to lesion, the number of Y chromosome positive cells was subtracted from the total number of nuclei in the plaque. The difference reflects the number of resident vessel wall derived cells, for example SMCs, in the lesion.

TUNEL Staining.

Apoptosis in atherosclerotic plaques was detected by the Terminal deoxynucleotide transferase (TdT) mediated dUTP nick end labeling (TUNEL) method using the Apoptag peroxidase kit (Chemicon). Briefly, sections of the aortic sinus from chimeric mice were deparaffinized in xylenes, rehydrated through an ethanol series and digested in 20 ug/ml proteinase K for 1 hour at room temperature. After blocking endogenous peroxidase activity with 3% H₂O₂, sections were incubated with 10 ul of TdT enzyme and reaction buffer solution, coverslipped with 12 mm round coverslips and incubated for 1 hour at 37°C. The TdT reaction adds digoxigenin-labeled dUTP nucleotides to the DNA strand breaks that are associated with

apoptotic cell death. Digoxigenin is a plant protein not present in mammalian cells, limiting the possibility of false positive staining due to antibody cross reactivity. After stopping the reaction in a stop/wash buffer, sections were incubated with peroxidase conjugated-anti digoxigenin antibody. Sections were then incubated with the chromogenic substrate 3,3'-diaminobenzidine (DAKO Corp), followed by counterstaining with hematoxylin (1:40). Negative controls were performed by omitting the TdT enzyme on serial sections. Positive controls were performed by incubating serial sections with 1U DNase I (0.1U/ul, Fermentas) to cause DNA strand breaks. The number of TUNEL positive nuclei in the lesions and total nuclei counts were counted at 40X by light microscopy. Data are expressed as the percentage of TUNEL positive nuclei per section.

BrdU pulse labeling and measurement of fatty streak lesion size.

Macrophage accumulation into the fatty streak was assessed by BrdU pulse labeling.² Starting at 10-12 weeks of age, *Ddr1*^{+/+}; *Ldlr*^{-/-} and *Ddr1*^{-/-}; *Ldlr*^{-/-} mice were fed the atherogenic diet for 2 weeks, then given a single i.v. injection of BrdU (10 mg/ml, 0.2 ml volume) a thymidine analog with a short half life that is incorporated into newly synthesized DNA.^{2,3} The BrdU pulse results in the labeling of a cohort of proliferating cells in both the bone marrow and aortic intima at the time of the injection. Mice were sacrificed 2 or 24 hours later, by anesthetic overdose with 67 mg/kg xylazine and 333 mg/kg ketamine i.p. The vasculature was perfused at 100 mmHg with chilled saline followed by chilled 4% paraformaldehyde for 5 minutes. The aortic arch and heart were immersion fixed in 4% paraformaldehyde on ice for 1 hour, cleared of fat and adventitia, and the ascending aorta from the aortic sinus and including ostia of the brachiocephalic artery was isolated.

En face preparations of the ascending aorta were stained for BrdU. Vessels were washed in 0.1% Triton X-100 and 1% fetal bovine serum in PBS, then permeabilized in 10% DMSO/0.5% Triton x-100 for 30 minutes on an orbital shaker. After blocking endogenous peroxidase activity with 0.3% H₂O₂ for 30 minutes, vessels were treated with 555U DNase I (Invitrogen) for 1.5 hours at 37 °C and incubated with a biotinylated anti-BrdU monoclonal antibody (1:200 MD5215, Invitrogen) overnight at 4°C. The next day, vessels were washed and incubated with streptavidin-HRP (1:300) for 1 hour at room temperature followed by incubation with FITC-tyramide (1:50) according the manufacturer's instructions (Tyramide signal amplification (TSA), Perkin Elmer). Counter staining of nuclei and lipids was performed using Hoescht 33528 (1:10000 in distilled H₂O) and Oil red O, respectively.

The total number of BrdU positive cells in the ascending aorta was counted using an Olympus Fluoview confocal microscope with a 60X oil immersion lens. As previously reported, BrdU positive cells cannot be detected in the circulation at 2 hours,² therefore the number of BrdU positive cells in the aortic intima at 2 hours provides a baseline measurement of intimal macrophage proliferation. In contrast, between 6 and 24 hours, there is a detectable cohort of BrdU positive monocytes present in the circulation (reference 10). Therefore, an increase in the BrdU positive cell number in the aortic intima between 2 and 24 hours reflects the appearance of newly labeled monocyte/macrophages in the developing fatty streak by a combination of local proliferation and recruitment from the circulation over a 22 hour time period. The number of BrdU positive cells per ascending aorta at each time point was expressed per unit of fatty streak lesion surface area to account for differences in lesion size between groups.

Since the lipid levels in these early plaques were too low to allow measurement of atherosclerotic plaque area by light microscopy, but Oil red O does fluoresce brightly, we exploited the increased sensitivity of Oil red O fluorescence to quantify fatty streak lesion size in these mice. Low magnification images of the *en face* preparations of ascending aorta were captured using a Biorad confocal microscope with a 4X objective. Images were captured at 543

nm excitation / 619 nm emission to detect the Oil red O stained lipid and 488 nm excitation / 519 nm emission to detect the autofluorescence of the internal elastic lamina. Measurement of the percentage of aortic surface area occupied by plaque was carried out using Simple PCI quantitative imaging software.

Flow Cytometry.

Ddr1^{+/+};Ldlr^{-/-} or *Ddr1^{-/-};Ldlr^{-/-}* mice fed the atherogenic diet for 2 weeks were pulse labeled with BrdU for 24 hours, and samples of peripheral blood (100ul) or bone marrow (10^6 cells) were taken to measure intracellular staining of BrdU using a flow cytometry (FITC-BrdU flow kit, Becton Dickinson) according to the manufacturer's instructions. Co-staining for monocytes in peripheral blood was performed using the following markers: CD115-phycoerythrin (PE, 1:100, eBioscience), Ly6C-biotin (1:200, BMA) and Streptavidin-allophycocyanin (SA-APC, 1:800, Becton-Dickinson). Samples were analyzed on a Beckman Coulter FC500 flow cytometer at the following wavelengths: FITC: 510 nm – 540 nm, PE: 560 nm – 590 nm, APC: 660 nm – 690 nm.

Peritoneal Macrophage Infiltration Assay.

In order to investigate macrophage infiltration into the peritoneum, *Ddr1^{+/+};Ldlr^{-/-}* and *Ddr1^{-/-};Ldlr^{-/-}* mice (n=8), were injected with 1 ml of 4% brewers modified thioglycollate medium (BD) in the peritoneal cavity, and 24 hours later were subjected to a peritoneal lavage with 10 ml RPMI. From the total lavage, aliquots of 10^6 cells in 1% BSA in RPMI were then incubated with unlabeled mAb or directly conjugated primary mAb for 30 min on ice. Staining was carried out using the following markers: CD115-phycoerythrin and Ly6C-biotin. Concentrations were the same as described above. Samples were analyzed on a Beckman Coulter FC500 flow cytometer as described above. Cells that were CD115+/LY6C+ were considered to be macrophages.

Macrophage adhesion assay.

Peritoneal macrophages were harvested from *Ddr1^{+/+};Ldlr^{-/-}* or *Ddr1^{-/-};Ldlr^{-/-}* mice by peritoneal lavage with cold RPMI, 4 days after i.p. injection of 1 ml sterile 4% brewer modified thioglycollate medium (BD) and a cell count was performed using a hemocytometer. 96 well plates were coated with 400nM of type IV collagen in a total volume of 50ul, incubated for 1 hour at 37° C to allow the collagen to reconstitute, and then left overnight at 4° C. 1×10^5 cells in 200 ul RPMI were added to the collagen-coated wells and cells were allowed to adhere for 2 hours at 37°C. Non adherent cells were rinsed off with PBS; adherent cells were fixed with 4% paraformaldehyde and stained with 0.5% toluidine blue. The absorbance of the solution in the well was measured in a microtiter plate reader (Molecular Devices, Sunnyvale, California, USA) at 595 nm. This experiment was repeated three times using macrophages isolated from 3 separate mice of each genotype.

Macrophage invasion assay.

Peritoneal macrophages were harvested from *Ddr1^{+/+};Ldlr^{-/-}* or *Ddr1^{-/-};Ldlr^{-/-}* mice by peritoneal lavage with cold RPMI, 3 days after i.p. injection of 1 ml sterile 4% brewer modified thioglycollate medium (BD). Harvested cells were cultured in DMEM containing 10% FCS and 2% penicillin/streptomycin for 24 hours prior to use in a macrophage invasion assay. Briefly, 8 µm transwell filters (Co-star) were coated with 100 ul of a 100 ug/ml collagen IV solution (Sigma), which was allowed to gel for 1 hour at 37 °C. Macrophages (10^5 cells/ well) suspended in 250 ul DMEM containing 2% BSA (serum free medium), were placed in the upper chamber of the transwell which were then placed in 24 well plates containing either serum free medium or 10 ng/ml recombinant mouse MCP-1 (R&D Systems). Invasion was allowed to occur for 4 hours at 37 °C after which cells that had migrated through the filter were stained with Coomassie blue and

counted. Five randomly selected 200X fields were counted and averaged for each experiment. The number of cells migrating in response to MCP-1 was normalized to the number migrating toward BSA for each genotype. Data was then expressed as an invasion index relative to *Ddr1*^{+/+} macrophages. This experiment was repeated three times using macrophages isolated from 3 separate mice of each genotype.

Statistical analysis.

Data are presented as mean \pm SEM. All statistical analysis was carried out using Sigma Stat (SyStat Software Inc.). Pairwise comparisons between transplant groups or genotypes were performed using Student's t-test. Data that did not fit a normal distribution was analyzed by Mann-Whitney U test for non-parametric comparisons. BrdU pulse data was analyzed using a one way ANOVA with a Tukey post hoc analysis for pairwise comparisons. Statistical significance was determined at $p < 0.05$.

Reference List

1. Franco C, Hou G, Ahmad PJ, Fu EYK, Koh L, Vogel WF, Bendeck MP. Discoidin domain receptor 1 (*Ddr1*) deletion decreases atherosclerosis by accelerating matrix accumulation and reducing inflammation in low-density lipoprotein receptor-deficient mice. *Circ Res.* 2008;102:1202-11.
2. Jongstra-Bilen J, Haidari M, Zhu SN, Chen M, Guha D, Cybulsky MI. Low-grade chronic inflammation in regions of the normal mouse arterial intima predisposed to atherosclerosis. *J Exp Med.* 2006;203:2073-83.
3. Kriss JP, Revesz L, Tung L, Egloff S. The distribution and fate of bromodeoxyuridine and bromodeoxycytidine in the mouse and rat. *Cancer Res.* 1962;22:254-65.

Supplemental Table I: Body weight and plasma lipids in DDR1 chimeric mice.

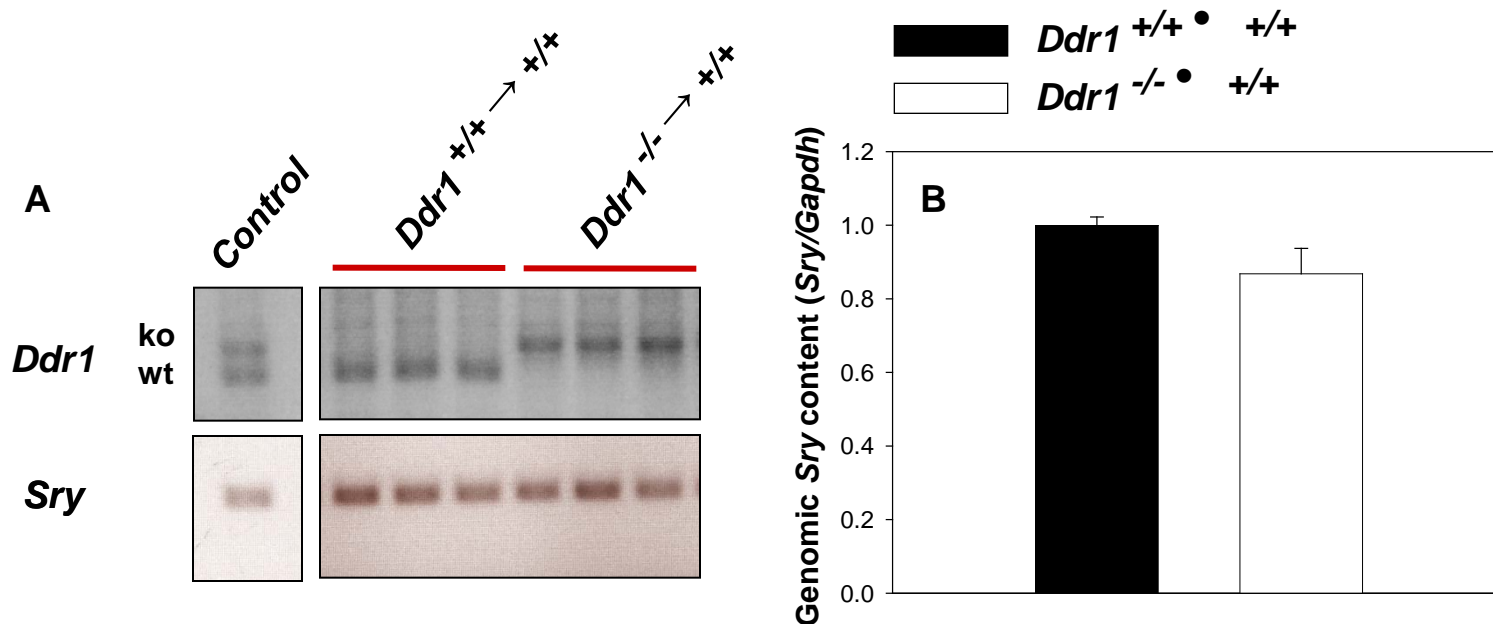
	<i>Ddr1</i> ^{+/+} → <i>+/+</i>	<i>Ddr1</i> ^{-/-} → <i>+/+</i>
Body Weight (g)	23.3 ± 2.4	25.6 ± 0.9
Total Cholesterol (mM)	12.6 ± 0.7	15.0 ± 0.9
Total Triglycerides (mM)	0.6 ± 0.1	0.6 ± 0.1

Supplemental Table I: Body weight and fasting plasma lipids in *Ddr1*^{+/+} → *-/-* and *Ddr1*^{-/-} → *+/+* chimeric mice. Body weight, fasting plasma cholesterol and triglycerides were measured after 12 weeks on the atherogenic diet.

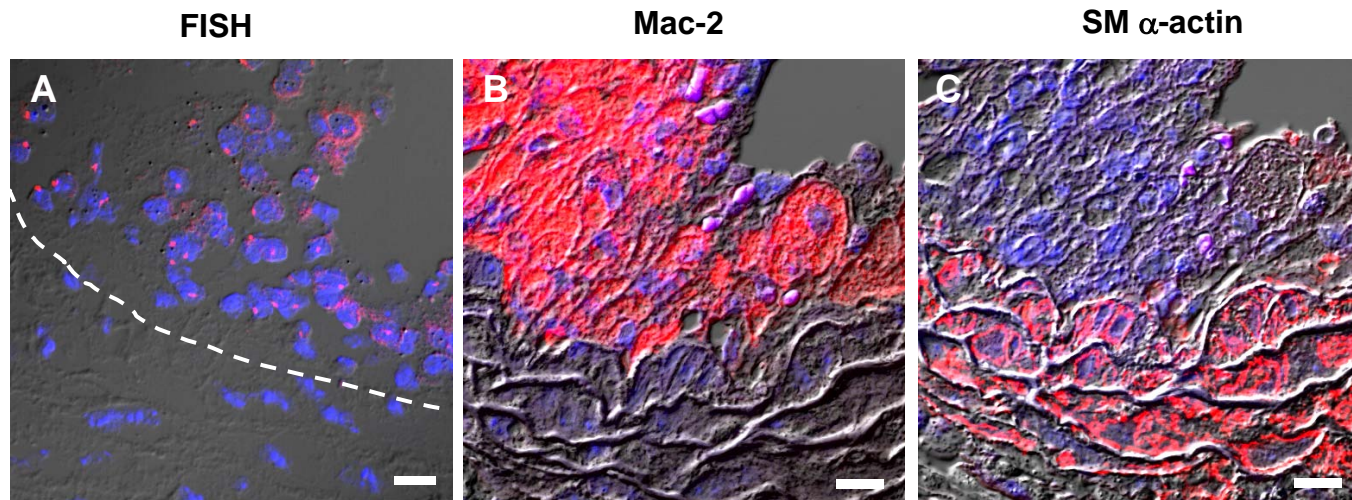
Supplemental Table II: Fasting plasma lipids in *Ddr1*^{+/+}; *Ldlr*^{-/-} and *Ddr1*^{-/-}; *Ldlr*^{-/-} mice.

	<i>Ddr1</i> ^{+/+} ; <i>Ldlr</i> ^{-/-}	<i>Ddr1</i> ^{-/-} ; <i>Ldlr</i> ^{-/-}
Total Cholesterol (mM)	31.3 ± 3.9	24.6 ± 1.7
Total Triglycerides (mM)	1.8 ± 0.3	1.4 ± 0.3

Supplemental Table II: Fasting plasma cholesterol and triglycerides were measured in *Ddr1*^{+/+}; *Ldlr*^{-/-} and *Ddr1*^{-/-}; *Ldlr*^{-/-} mice sacrificed after 2 weeks on the atherogenic diet.



Supplemental Figure I: Assessment of male:female chimerism after reciprocal bone marrow transplant. **(A)** Genomic DNA was isolated from peripheral blood of transplanted chimeric mice and was used to genotype for *Ddr1* and *Sry*, a marker of the Y chromosome. Control lane contains tail DNA from a *Ddr1*^{+/-} male mouse, with the upper band of the doublet representing the *Ddr1* knockout allele (ko) and the lower band representing the wild type allele (wt). Genotyping for DDR1 in chimeric mice demonstrated the presence of the donor DDR1 allele in leukocytes, with minimal presence of the host allele. The abundance of *Sry* was comparable in both groups. **(B)** Male chimerism was also measured by quantitative PCR for *Sry* and *Gapdh*. n=7 animals per group.



Supplemental Figure II: Correlative immunofluorescence to identify the cell type of bone marrow derived cells. Serial cross sections of the aortic sinus were immunostained with antibodies against Mac-2 and SM α -actin and confocal images were correlated with areas of plaque that were analyzed by FISH. Red indicates Y chromosome positive nuclei in the FISH image (A) and the immunofluorescent detection of Mac-2 (B) or SM α -actin (C). Nuclei were stained with Hoescht 33528 and are coloured blue. A grey DIC overlay was added to highlight lesion morphology. From this analysis we conclude that the majority of Y chromosome positive cells are macrophages.